

# CLEAR-IR: Clarity-Enhanced Active Reconstruction of Infrared Imagery for low-light enhancement

Nathan Shankar<sup>id</sup>, Marton Gonczy<sup>id</sup>, Hujun Yin<sup>id</sup>, and Pawel Ladosz<sup>id</sup>

**Abstract**—This paper presents a novel approach for enabling robust robotic perception in dark environments using infrared (IR) stream. IR stream is less susceptible to noise than RGB in low-light conditions. However, it is dominated by active emitter patterns that hinder high-level tasks such as object detection, tracking and localisation. To address this, a Deep Multi-scale Aware Overcomplete (DeepMAO) inspired architecture is proposed that reconstructs clean IR images from emitter populated input, improving both image quality and downstream robotic performance. This approach outperforms existing enhancement techniques and enables reliable operation of vision driven robotic systems across illumination conditions from well-lit to extreme low-light scenes. The results outline the ability of this work to be able to mimic RGB styling from the scene and its applicability on robotics tasks that were trained on RGB images, opening the possibility of doing these tasks in extreme low-light without on-board lighting.

**Index Terms**—Infrared Imaging, Image Reconstruction, U-Net, Low-Light Perception, Computer Vision, Robotics

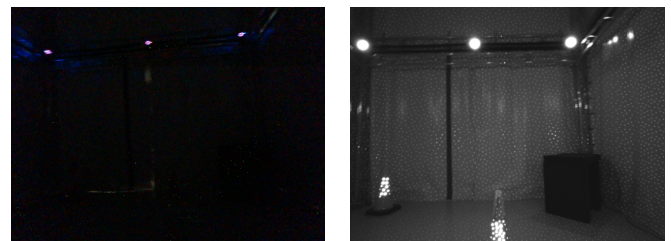
## I. INTRODUCTION

Lighting-invariant vision systems are desirable for enabling robots to operate robustly across diverse and unpredictable environments without requiring modifications to the underlying perception pipeline. In order to support high-level tasks such as object detection, semantic segmentation, and image classification, the vision system must remain reliable even in low light or completely dark scenes. Such capabilities are critical in domains like mine shaft exploration, post-disaster victim identification, nuclear facility inspection, and visual loop closure in feature-deprived environments using aruco markers.

Conventional RGB cameras, while effective under well-lit conditions, suffer from significant degradation in low-light scenes [1]. Image quality is compromised due to sensor-level limitations, such as dark current and readout noise. Attempts to compensate using an increased exposure time introduce motion blur, rendering them ineffective for dynamic environments. Furthermore, data-driven approaches relying solely on visible spectrum low light and long exposure pairs are fundamentally limited by information-theoretic constraints. If critical scene information is not captured by the sensor due to extreme darkness or sensor level noise, it cannot be reconstructed regardless of the training data volume. Consequently, the efficacy of these networks remains strictly

bound by the inherent observability of the visible spectrum in degraded conditions.

Another approach involves equipping robots with onboard illumination systems [2]. However, in certain rich environments such as underground tunnels or disaster zones, the Tyndall effect causes the light to scatter off airborne particles, saturating the camera view with undesirable visual artefacts and occluding key features in the scene. This method also suffers from overexposure, specular reflection, and increased power consumption. Moreover, the use of active illumination can produce strong shadows that obscure structural details and complicate downstream vision tasks such as object detection and localisation. To address these challenges, this work explores the use of infrared (IR) imaging, particularly active IR systems that operate independently of ambient illumination. As seen in Figure 1, the dark scene captured by the RGB camera fails to present good visual cues, whereas the same scene in the IR spectrum can be visualised with several objects in the scene. Although IR cameras are less susceptible to such scattering due to its longer wavelength and are promising for dark-scene perception, they are not without their own limitations. Passive IR sensors, which operate without emitters, avoid structured-light artefacts but are typically expensive and limited to low-resolution outputs. Conversely, active IR systems often rely on structured light or flash patterns, and while these provide better penetration through dusty scenes than having an ambient light in extreme low-light scenes, the resulting high-intensity reflections and projected patterns can interfere with feature extraction, and disrupt downstream perception tasks such as object detection and Simultaneous Localisation and Mapping (SLAM).



(a) Low-light room captured using an RGB camera (b) Low-light room captured using an IR camera

Fig. 1: Low-light room captured using different cameras

To overcome this, a deep learning-based framework, CLEAR-IR (Clarity-Enhanced Active Reconstruction of Infrared Imagery), is proposed. The framework is designed

This work was supported by Robotics and Artificial Intelligence Collaboration (RAICo). (Corresponding author: Pawel Ladosz.) The authors are with the the Mechanical, Aerospace and Civil Engineering and the Electrical and Electronics Departments at the University of Manchester, Manchester, United Kingdom, M13 9PL. (e-mail: nathan.shankar@postgrad.manchester.ac.uk).

to reconstruct clean and interpretable IR images from raw emitter populated inputs. The method leverages a Deep Multi-scale Aware Overcomplete (DeepMAO [3]) inspired architecture trained to suppress structured light noise while preserving spatial and textural details critical for vision-based tasks. The output is a reconstructed, visually coherent IR image that can serve as a robust input to standard perception modules. This is the first work to leverage the infrared stream for high-level robotic tasks by removing active emitter patterns in scenes ranging from well-illuminated to extreme low-light. The contributions of this work are:

- CLEAR-IR, a DeepMAO inspired architecture tailored for reconstructing clean IR images by suppressing structured-light artefacts, is introduced.
- We utilise a composite loss function specifically selected to accommodate the spectral disparity and lack of pixel perfect alignment between IR and RGB inputs, allowing for robust pattern removal while preserving details critical for robotic perception.
- Evaluation of IR image reconstruction for robotics is presented, demonstrating significant improvements across key tasks such as object detection and marker detection.
- Comparison with other SOTA techniques for localisation in extreme low-light scenes.

## II. RELATED WORK

Vision-based robotic perception in challenging lighting conditions has been an active area of research. One line of work has focused on improving the performance of standard RGB cameras in low light. This includes sensor-level enhancements such as improved read-out noise reduction and pixel architectures [4], as well as computational photography techniques such as multiexposure fusion [5] and burst photography [6]. Although these techniques can improve image quality, they are often computationally intensive and can introduce motion blur or require static scenes, limiting their use in dynamic robotic applications.

A separate body of work leverages deep learning for low-light image enhancement. Prominent examples include supervised learning methods that train neural networks on paired low light and well lit images [7], [8]. These approaches, however, are highly dependent on the quality and diversity of the training data and may not generalise well to different camera hardware or unseen environments. Unsupervised and semi-supervised methods have also been explored to mitigate the need for paired data as seen in [9]–[11], but they often struggle to remove complex artefacts such as structured light patterns found in active IR systems, which this work explores. Generative adversarial networks (GANs) have been used for enhancement in low light as inferred from [12]–[14], but these methods do not translate well to extremely low light scenes, which require some form of active sensing. Moreover, the artefacts introduced by these methods are particularly problematic for robotics: vision-based SLAM pipelines may incorrectly latch onto these artificial structures as features, leading to spurious correspondences, tracking

drift, and eventual map corruption. Thus, preserving fine-grained but genuine details is critical for ensuring robustness in downstream tasks such as vSLAM and visual odometry.

Active infrared (IR) systems provide a robust alternative for dark-scene perception by illuminating the environment with a dedicated source. While high power IR floodlights offer uniform coverage, they are often impractical for mobile robotics due to the inverse-square law, the power required for an adequate signal-to-noise ratio scales quadratically with distance. Furthermore, floodlights frequently cause shadows and also severe near-field saturation, where excessive photon flux annihilates local contrast and occludes critical features. To mitigate this while providing the structural texture necessary for navigation on featureless surfaces, depth camera manufacturers utilise structured-light or modulated laser patterns [15]. Beyond their sensing advantages, these active IR systems are already standard components in many robotic platforms and leveraging them for 2D perception minimizes system complexity, reduces payload weight, and lowers maintenance costs compared to adding auxiliary illumination hardware. By distributing energy into discrete, evenly spaced points, these systems maintain a higher usable dynamic range even as pattern density increases at close proximity, the localised nature of the emission prevents the global washout characteristic of floodlights. However, these high-frequency patterns present a significant challenge for 2D vision tasks, as standard algorithms often misinterpret them as scene texture, leading to false detections. Previous denoising works [16]–[18] focus primarily on removing static sensor level artefacts rather than addressing the dynamic, pattern dependent noise inherent to these active emitters. Simply enhancing these inputs does not bridge the domain gap required for robotics, as static corrections cannot account for the characteristics discussed in Section III-A.

The U-Net architecture, with its symmetric encoder-decoder structure, skip connections, has shown remarkable success in a variety of image-to-image translation tasks, and was first introduced for biomedical image segmentation in [19]. Its ability to capture both high-level semantic information from the encoder path and fine-grained spatial details from the decoder path makes it an ideal candidate for the specific reconstruction problem encountered in IR images. This architecture has also been successfully adapted for other image reconstruction tasks, such as super-resolution [20] and general image denoising [21].

In contrast to existing methods that primarily focus on low-light enhancement or general noise removal, this work addresses the specific and unique problem of structured light artefacts in active IR imagery. Using the DeepMAO architecture, it is possible to effectively learn to suppress these specific patterns while preserving the crucial underlying semantic information for high-level vision tasks.

## III. METHODOLOGY

This section presents the CLEAR-IR framework. Unlike standard encoder-decoder approaches, CLEAR-IR uses a hybrid dual-branch architecture to effectively remove structured

light artefacts while preserving critical visual details.

### A. Emitter Pattern Characteristics

Active infrared (IR) systems enable vision in dark environments by projecting an illumination pattern onto the scene. This pattern is often a pseudo-random pattern which is a semi-deterministic and repeatable sequence of dots generated by an algorithm. The raw IR image captured by the camera is, therefore, populated with these dots, which can be misidentified as texture or objects by standard vision algorithms, complicating tasks like object detection and segmentation.

The intensity of these dots in the captured image is not uniform and depends on four main factors:

- **Object Reflectivity:** Objects with higher reflectivity in the IR spectrum will appear brighter, as they reflect a sharper emitter pattern to the camera, as shown in Figure 2a, where the plastic screen reflects more emitter pattern than the black foam.
- **Distance to the Emitter:** The intensity of the light from the emitter decreases with the square of the distance, following the inverse square law. Consequently, closer objects will show a more intense and prominent dot pattern, where the patterns are larger when closer and smaller when they move further away from the camera, as seen in Figure 2b and Figure 2a, where the closer part of the sheet has more shaper patterns than the further part.
- **Emitter Power:** The overall intensity of the pattern is directly proportional to the laser power of the emitter, where a higher power leads to a denser, more defined pattern. This is also a critical factor in the appearance of the pattern, as seen in Figure 2c, where a lower laser power prevents the room from being seen while a larger laser power populates the room with the emitter pattern.
- **Room Brightness:** This factor contributes to the emitter power configuration, where the same emitter pattern may appear dimmer in well-illuminated scenes while appearing sharper in low-light scenes, as seen in Figure 2d and Figure 2e, where ambient light affects the emitter visibility by dimming the laser power.

This variability in pattern appearance across different scenes poses a challenge in selecting adequate losses that can remove them from the images while being scene agnostic.

### B. CLEAR-IR Architecture

To preserve high-frequency spatial details, this work adopts a modified DeepMAO architecture. Although the original DeepMAO was modelled for satellite image segmentation using a pretrained EfficientNet backbone along with a combination of focal loss and dice loss, this work adapts its dual-stream ideology for IR image reconstruction. This work simplifies the original architecture by replacing the heavy encoder with a U-Net backbone and we simplify the multi-scale overcomplete (MSO) module from non-integer interpolations to a sequence of full-resolution convolution layers. We retain the original architecture’s additive residual

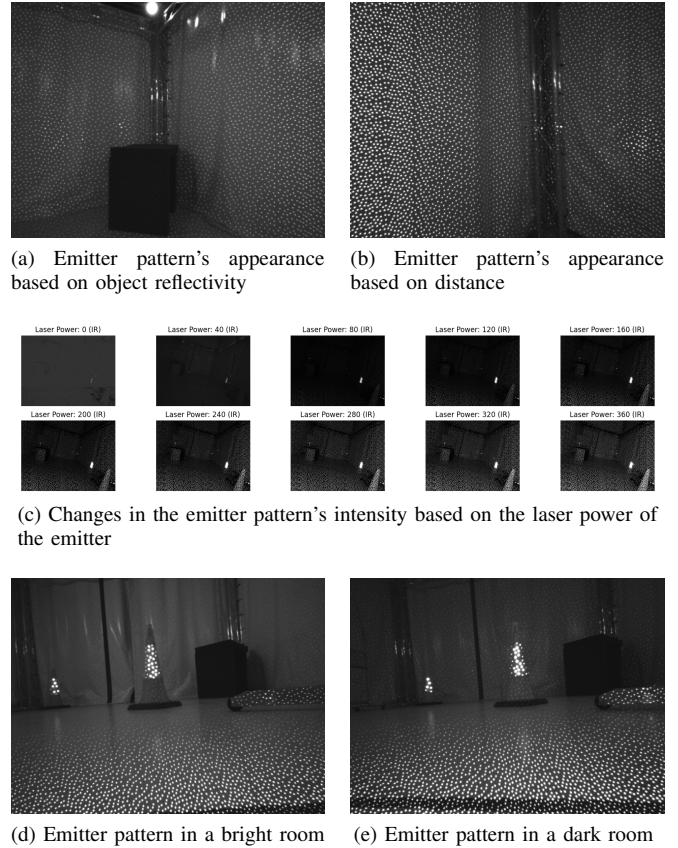


Fig. 2: The key factors influencing the appearance of the structured light emitter pattern in active infrared imagery.

fusion to facilitate a direct gradient flow for fine-grained textures. Furthermore, we transition the training objective from pixel-level classification to intensity regression, utilising a combined perceptual and structure loss tailored for scene reconstruction.

1) *Context Stream (U-Net Backbone):* Unlike the original DeepMAO which relied on a heavy EfficientNet-B3 encoder, our first branch utilises a U-Net backbone designed to efficiently capture global context and low-frequency structural information.

- **Hierarchical Encoding:** The encoder processes the input through a series of convolutional blocks with increasing filter depths (32, 64, 128) and  $2 \times 2$  max-pooling layers. This effectively expands the receptive field, allowing the network to understand global scene geometry.
- **Regularisation:** To ensure stability during training and prevent overfitting on specific emitter patterns, dropout with a rate of 0.2 is integrated into the deeper layers of the encoder and bottleneck.
- **Decoder and Skip Connections:** The decoder utilises transposed convolutions to upsample feature maps, concatenated with corresponding features from the encoder to recover spatial information lost during pooling.

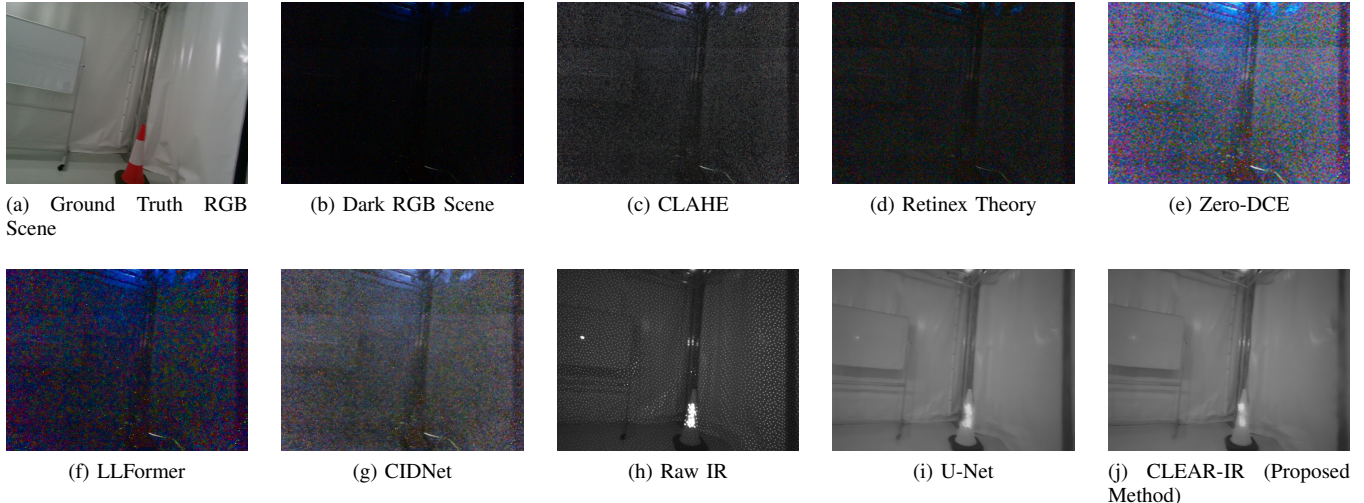


Fig. 3: Visual comparison of enhancement methods on example scene.

2) *Detail Stream (Overcomplete Branch)*: While the pooling operations in the U-Net are effective at smoothing out the artificial structured light patterns, they are also destructive to the true high frequency details of the scene. To mitigate this, the second branch acts as an overcomplete pathway.

- **Full Spatial Resolution**: In the original DeepMAO, the overcomplete path utilized complex non-integer interpolations and dilated convolutions. We simplify this mechanism to better suit image reconstruction. Our branch accepts the initial feature maps (32 filters) and processes them through a cascade of convolutional layers without any scaling, pooling, or strided operations.
- **Detail Preservation and Noise Suppression**: By strictly maintaining a 1:1 input-to-output spatial correspondence, this branch bypasses the destructive down-sampling of the U-Net. It specialises in isolating the true high-frequency structural boundaries from the structured light noise, ensuring that sharp edges and fine scene textures are preserved and injected back into the final reconstruction.

3) *Feature Fusion*: The outputs of the U-Net branch and the spatial overcomplete branch are integrated using an additive fusion strategy, mirroring the residual nature of the original network.

$$F_{fused} = F_{unet} \oplus F_{overcomplete} \quad (1)$$

where  $\oplus$  denotes element-wise addition. This residual-style fusion allows the network to combine the clean structural predictions from the U-Net with the texture corrections from the overcomplete branch. The fused features are passed through a final convolutional refinement block to generate the continuous intensity values of the reconstructed IR image.

### C. Loss Function

Despite the extrinsic calibration and warping process, minor alignment residuals persist due to parallax and sensor baseline between the IR and RGB camera. Therefore,

this work uses a composite loss function that prioritises perceptual quality and structural integrity over simple pixel-wise accuracy. The total loss  $\mathcal{L}_{total}$  is a weighted sum of six components:

$$\begin{aligned} \mathcal{L}_{total} = & \alpha \mathcal{L}_{mae} + \beta \mathcal{L}_{ssim} + \gamma \mathcal{L}_{freq} \\ & + \delta \mathcal{L}_{sobel} + \epsilon \mathcal{L}_{perceptual} + \zeta \mathcal{L}_{tv} \end{aligned} \quad (2)$$

The components are defined as follows:

- **Spatial Fidelity** ( $\mathcal{L}_{mae}, \mathcal{L}_{ssim}$ ): This work use Mean Absolute Error (MAE) for base intensity matching and Structural Similarity Index (SSIM) [22] to preserve luminance and contrast structure.
- **Detail Preservation** ( $\mathcal{L}_{freq}, \mathcal{L}_{sobel}$ ): To retain sharp edges,  $\mathcal{L}_{freq}$  minimizes the  $L_1$  distance between Laplacian-filtered images, while  $\mathcal{L}_{sobel}$  penalizes discrepancies in image gradients.
- **Perceptual Quality** ( $\mathcal{L}_{perceptual}$ ): A VGG19 network pre-trained on ImageNet [23] is used as a feature extractor. The loss minimises the  $L_1$  distance between feature maps of specific intermediate layers, ensuring the reconstruction aligns with human visual perception [24]:
- **Regularization** ( $\mathcal{L}_{tv}$ ): Total Variation (TV) loss promotes spatial smoothness to reduce spurious noise in uniform regions.

The weighting coefficients ( $\alpha, \beta, \gamma, \delta, \epsilon, \zeta$ ) were experimentally tuned to prioritize  $\mathcal{L}_{ssim}$  and  $\mathcal{L}_{perceptual}$ , ensuring the model focuses on structural removal of the pattern rather than overfitting to minor pixel misalignments.

### D. Data Augmentation and Training Implementation

A custom dataset was developed by capturing 6,719 initial pairs of active IR and greyscale RGB images using an Intel RealSense D455 camera [25]. To ensure spatial correspondence, we utilised factory calibrated extrinsics to align the sensors. These base frames were diversified through data

augmentation, including random rotations ( $\pm 30^\circ$ ), flipping, affine transformations, and brightness adjustments resulting in a final dataset of 33,595 images. The model was trained to map IR inputs to an RGB-style ground truth, enabling the deployment of downstream vision tasks originally developed for the visible spectrum. The network was trained on a 90 to 10 data split at  $640 \times 480$  resolution using the Adam optimizer with a cosine decay scheduler. Early stopping was also used to ensure convergence while preventing overfitting.

#### IV. EXPERIMENTAL RESULTS

This section presents a comprehensive evaluation of the proposed CLEAR-IR framework, focusing on its effectiveness in preparing infrared images for high-level computer vision tasks. Since this is the first work to specifically address the removal of active emitter patterns, the primary evaluation is a qualitative and quantitative comparison of the performance of enhancement techniques on the RGB stream versus the reconstructed images of the IR stream produced by this work.

The advantages of the CLEAR-IR method is emphasised through a quantitative comparison against both traditional baselines and a diverse set of state of the art (SOTA) enhancement methods. We evaluate against classical spatial-domain techniques, including CLAHE [26] and retinex theory inspired methods [27]. To benchmark against modern deep learning advances, this work evaluates Zero-DCE [28], a zero-reference method for unsupervised curve estimation, LLFormer [29], a benchmark Transformer-based architecture optimised for long-range dependency modelling and CIDNet [30], a multi-axis decoupling network that utilises a new HVI colour space to suppress colour bias and noise. These methods provide a robust evaluation across the leading unsupervised, attention-based, and colour-decoupling methodologies.

The visual results in Figure 3 shows the outputs from different techniques on an unknown scene. While other methods attempt to enhance the image, the enhanced RGB images are affected by the effects of noise observed in low-light scenes. The IR cameras are more robust to the effect of this noise in low-light, as a result, the CLEAR-IR framework produces a clean, artifact free image that maintains the scene’s structural integrity without introducing any additional artefacts or hallucinating. This demonstrates that the proposed method is more effective at generating a representation of the scene suitable for downstream vision tasks.

Beyond the general quality metrics, the true utility of the proposed CLEAR-IR framework is demonstrated by its ability to facilitate high-level robotics tasks that are otherwise compromised by the structured light patterns and noise inherent in raw IR images and RGB images respectively. Table I presents a comprehensive quantitative comparison of the performance of various image enhancement methods on high level tasks such as object detection, and ArUco marker detection. The results highlight a critical distinction between methods that simply improve image aesthetics and those that produce a robust, clean representation suitable for

downstream algorithms. The proposed work is also used in feature tracking and odometry estimation to highlight the stability across frames in unseen environments.

##### A. Object Detection and Segmentation

To demonstrate the utility of the reconstructed images for advanced perception tasks, a pre-trained YOLOv26 object detection and segmentation model was used for evaluation. This model was not trained on IR data, making this a zero-shot evaluation to determine if the proposed preprocessing step can make the images usable with standard RGB-based vision pipelines.

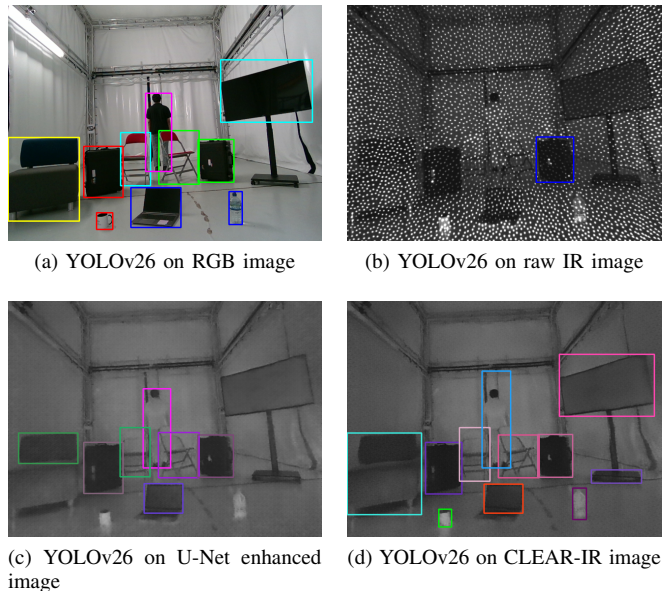


Fig. 4: Object detection and segmentation results of YOLOv26 on raw and reconstructed IR images.

On the raw IR images, YOLOv26 failed to detect or segment objects. The emitter patterns and resulting image noise prevented the model from recognising the distinct shapes and features of common objects. After preprocessing the images with the CLEAR-IR model, the performance of YOLOv26 dramatically improved. As illustrated in Figure 4, the model successfully detected and segmented objects in the reconstructed images, which were completely missed in the raw inputs. While tested on a variety of images, some labels were incorrect since the YOLOv26 model had not been trained on the specific objects present in the scene. For example, traffic cones were occasionally misclassified as bottles, and a white storage cabinet was misclassified as a refrigerator. Although the greyscale nature of IR data makes some misclassification inevitable without fine-tuning. Importantly, despite some label mismatches, the model was able to consistently detect and track these objects across frames, demonstrating the usability of CLEAR-IR outputs for object-level perception.

TABLE I: Performance comparison of image enhancement methods for various computer vision tasks.

Method	Object Detection (Visible Objects)			ArUco Marker Detection	
	Detected	Missed	Mislabelled	Correct	Missed
Retinex Theory [27]	1	9	0	5	1
CLAHE [26]	1	9	0	3	3
Zero-DCE [28]	0	10	0	5	1
LLFormer [29]	0	10	0	5	1
CIDNet [30]	1	9	0	<b>6</b>	<b>0</b>
Raw IR	0	9	1	0	6
U-Net	<b>7</b>	<b>3</b>	<b>0</b>	<b>6</b>	<b>0</b>
CLEAR-IR (Proposed Method)	<b>11</b>	<b>0</b>	<b>2</b>	<b>6</b>	<b>0</b>

### B. ArUco Marker Detection

ArUco markers are fiducial markers widely used in robotics for localisation and pose estimation. The ability to reliably detect these markers is crucial for robust navigation. However, structured light patterns can interfere with the marker’s distinct black-and-white grid, often leading to detection failures. This interference is clearly visible in the raw infrared (IR) image shown in Figure 5b. For comparison, a baseline for successful detection is provided by the standard RGB image, as seen in Figure 5a.

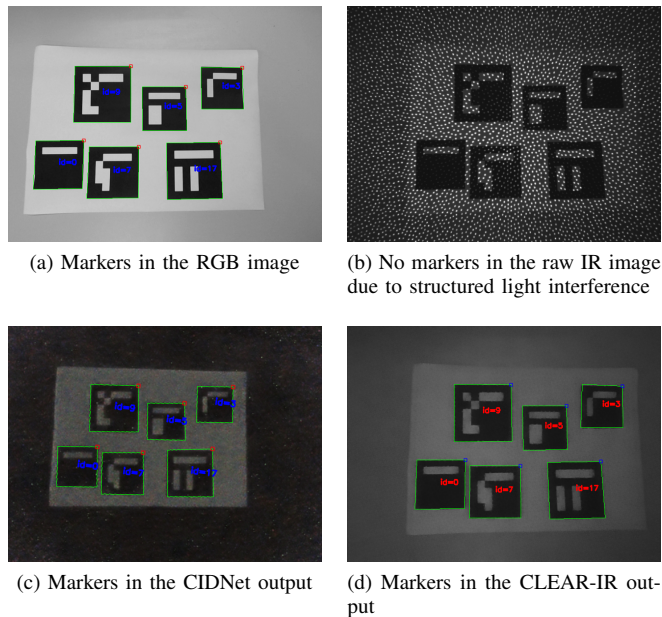


Fig. 5: Comparison of ArUco marker detection performance on RGB, raw IR, and reconstructed IR images.

The CLEAR-IR framework addresses these challenges by enabling robust ArUco marker detection in IR images. By removing the spurious dot patterns, the model ensures the marker’s grid is clearly visible and interpretable by the detection algorithm, as demonstrated in Figure 5d. This is a significant advancement for low-light scenes where raw IR images are typically unusable for this task. The reconstructed output allows for consistent and accurate marker identification, thus enabling reliable localisation and mapping. This outcome directly contrasts with findings in prior work, such

as [31], which concluded that raw IR images were unsuitable for low-light tag detection without the use of retroreflective materials. Similarly, this approach simplifies methods like [32], which propose using specialised tags for low-light localisation, by requiring no special tags or materials.

### C. Visual Simultaneous Localisation and Mapping (VSLAM) Performance

To evaluate the practical utility of CLEAR-IR for robotics applications, we integrated the reconstructed infrared stream into a modified ORB-SLAM3 [33] Visual SLAM pipeline. In our implementation, the default ORB feature extractor was replaced with SuperPoint [34], and feature matching was adapted accordingly to use floating-point descriptor matching with L2 distance. This modification ensures compatibility with learned feature descriptors while preserving the full SLAM pipeline, including tracking, local mapping, and loop closure. Robust SLAM performance critically depends on stable and repeatable feature tracking across frames. In raw IR images, however, the structured light emitter pattern introduces dense artificial high-frequency responses. These phantom features are inconsistent across viewpoints and frames, leading to incorrect correspondences, tracking divergence, and eventual tracking failure. This behaviour is reflected in the Table II where Raw IR fails in all sequences.

To ensure fair comparison with RGB-based enhancement methods, monocular RGB and depth sequences were recaptured under controlled lighting conditions. Three trajectories were recorded:

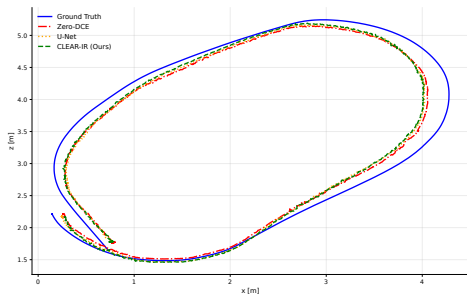
- Forward-Backward (FB): This sequence is a simple movement of moving in a straight line till an object and reversing backward
- Square 1 lap (SQ1): This sequence is a simple movement of rotating along an arena and returning to the start point as seen in Figure 6.
- Square 2 lap (SQ2): This sequence repeats the SQ1 trajectory for two full laps, providing a benchmark for observing the model’s ability to facilitate successful loop closure and drift correction

Table II reports results in low-light conditions where limited ambient illumination is still present. Under these conditions, the RGB enhancement methods (Retinex, CLAHE, Zero-DCE, LLFormer, CIDNet) perform reliably because the RGB images retain sufficient structural information for feature extraction and tracking. CLEAR-IR and the U-Net base-

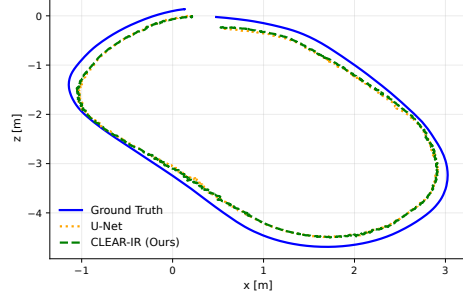
TABLE II: Quantitative evaluation of SLAM trajectory accuracy (RMSE in meters) and inference latency across Low Light (LL) and Extreme Low Light (ELL) scenarios.

Method	Low Light (LL) - RMSE $\pm$ std			Extreme Low Light (ELL) - RMSE $\pm$ std			Inference (ms)	
	FB	SQ1	SQ2	FB	SQ1	SQ2	Mean	std
Retinex [27]	<b>0.064<math>\pm</math>0.02</b>	0.163 $\pm$ 0.05	0.168 $\pm$ 0.05	DNI	DNI	DNI	73.43	10.54
CLAHE [26]	0.069 $\pm$ 0.03	0.156 $\pm$ 0.05	0.169 $\pm$ 0.05	DNI	DNI	DNI	<b>15.16</b>	<b>3.09</b>
Zero-DCE [28]	0.065 $\pm$ 0.02	<b>0.147<math>\pm</math>0.05</b>	0.190 $\pm$ 0.05	DNI	DNI	DNI	46.35	2.32
LLFormer [29]	0.067 $\pm$ 0.03	0.156 $\pm$ 0.05	0.183 $\pm$ 0.05	DNI	DNI	DNI	236.88	10.20
CIDNet [30]	0.069 $\pm$ 0.03	0.560 $\pm$ 0.22	0.178 $\pm$ 0.05	DNI	DNI	DNI	76.33	0.86
Raw IR	DNI	DNI	DNI	DNI	DNI	DNI	DNI	DNI
U-Net	0.072 $\pm$ 0.03	0.161 $\pm$ 0.06	0.164 $\pm$ 0.06	0.097 $\pm$ 0.05	0.167 $\pm$ 0.05	0.168 $\pm$ 0.06	49.93	3.42
<b>CLEAR-IR (Ours)</b>	0.070 $\pm$ 0.03	0.164 $\pm$ 0.06	<b>0.137<math>\pm</math>0.07</b>	<b>0.092<math>\pm</math>0.04</b>	<b>0.159<math>\pm</math>0.05</b>	<b>0.159<math>\pm</math>0.12</b>	46.75	3.48

DNI: Did Not Initialise; Bold shows best results



(a) SQ1 trajectories in the low-light sequence



(b) SQ1 trajectories in the extreme low-light sequence

Fig. 6: Square 1 lap (SQ1) Trajectories

line achieve performance comparable to these RGB-based methods. In simpler trajectories (FB and SQ1), CLEAR-IR performs on par with the RGB enhancement models. Notably, in the SQ2 sequence, CLEAR-IR achieves the lowest RMSE among all evaluated methods. Since SQ2 stresses loop closure and long-term consistency, this result indicates that CLEAR-IR reconstructs temporally stable structures that reduce drift accumulation over extended trajectories. Importantly, unlike raw IR, the reconstructed outputs do not introduce false high-frequency artefacts from the emitter pattern. Instead, the learned reconstruction produces geometrically meaningful and temporally consistent features suitable for SLAM.

Furthermore in extreme low-light conditions the RGB images become severely underexposed, containing insufficient texture or gradient information for reliable feature detection. Consequently, all RGB-based enhancement methods fail to maintain tracking across every sequence, as indicated by missing RMSE values. In contrast, the IR images remain unaffected by ambient lighting conditions. While raw IR still fails due to emitter induced phantom features, both U-Net and CLEAR-IR successfully enable full SLAM operation across all sequences. CLEAR-IR consistently outperforms the U-Net baseline in terms of RMSE, achieving the best accuracy in FB, SQ1, and SQ2. This demonstrates a key advantage of the proposed framework: when RGB information collapses, CLEAR-IR leverages the invariant structural

information present in the IR modality to reconstruct geometrically consistent representations that remain usable for feature-based SLAM. In terms of inference latency, CLEAR-IR maintains competitive runtime performance. While classical methods such as CLAHE are significantly faster, they do not provide robustness under extreme lighting degradation. Conversely, transformer-based models such as LLFormer incur substantially higher computational cost. CLEAR-IR achieves a favourable trade-off between localisation accuracy and inference speed, maintaining compatibility with real-time SLAM update requirements.

## V. CONCLUSION

Utilising the infrared cameras already commonly integrated into robotic systems, the CLEAR-IR framework effectively addresses a fundamental perception challenge by removing emitter patterns from infrared images, successfully enabling low-light vision and extending the use case of these camera systems. Leveraging a DeepMAO inspired architecture, the method produces visually coherent and artifact free outputs that are compatible with existing computer vision pipelines in a fully dark environment. The significance of this contribution is further evidenced by the substantial improvement in performance for downstream tasks, including VIO, object detection, and marker detection. As confirmed by quantitative results, this approach establishes a new standard, demonstrably surpassing state-of-the-art low-light RGB

enhancement techniques, showing flexibility even in entirely dark scenes. The CLEAR-IR framework thus provides a robust and reliable foundation for enabling autonomous systems to operate effectively in a wider range of challenging lighting conditions.

## VI. FUTURE DIRECTION

Future work will concentrate on two primary objectives to advance the CLEAR-IR framework's utility in practical applications such as enhancing computational efficiency and enabling robust integration with visual Simultaneous Localisation and Mapping (vSLAM) systems. To improve processing time, research will explore model optimisation techniques, such as network quantisation and model pruning.

## ACKNOWLEDGMENT

RAICo contributed to this work by providing funding and a supportive research environment. Jongyun Kim assisted the authors with setup and data collection in a dark environment.

## REFERENCES

- [1] X. Guo and Q. Hu, "Low-light image enhancement via breaking down the darkness," *International Journal of Computer Vision*, vol. 131, no. 1, pp. 48–66, 2023.
- [2] F. Crocetti, A. Dionigi, R. Brilli, G. Costante, and P. Valigi, "Active illumination for visual ego-motion estimation in the dark," in *2025 IEEE International Conference on Robotics and Automation (ICRA)*, 2025, pp. 14 087–14 093.
- [3] A. Sikdar, S. Udupa, P. Gurunath, and S. Sundaram, "Deepmao: Deep multi-scale aware overcomplete network for building segmentation in satellite imagery," in *Proceedings of the IEEE/CVF Conference on Computer Vision and Pattern Recognition*, 2023, pp. 487–496.
- [4] J. Ma, S. Chan, and E. R. Fossum, "Review of quanta image sensors for ultralow-light imaging," *IEEE transactions on electron devices*, vol. 69, no. 6, pp. 2824–2839, 2022.
- [5] Z. Ying, G. Li, and W. Gao, "A bio-inspired multi-exposure fusion framework for low-light image enhancement," *arXiv preprint arXiv:1711.00591*, 2017.
- [6] A. S. Karadeniz, E. Erdem, and A. Erdem, "Burst photography for learning to enhance extremely dark images," *IEEE Transactions on Image Processing*, vol. 30, pp. 9372–9385, 2021.
- [7] T. Chobola, Y. Liu, H. Zhang, J. A. Schnabel, and T. Peng, "Fast context-based low-light image enhancement via neural implicit representations," in *European Conference on Computer Vision*. Springer, 2024, pp. 413–430.
- [8] M. J. Reis, "Low-light image enhancement using deep learning: A lightweight network with synthetic and benchmark dataset evaluation," *Applied Sciences*, vol. 15, no. 11, p. 6330, 2025.
- [9] W. Yang, S. Wang, Y. Fang, Y. Wang, and J. Liu, "From fidelity to perceptual quality: A semi-supervised approach for low-light image enhancement," in *Proceedings of the IEEE/CVF conference on computer vision and pattern recognition*, 2020, pp. 3063–3072.
- [10] M. A. N. I. Fahim, N. Saqib, and H. Y. Jung, "Semi-supervised atmospheric component learning in low-light image problem," *Plos one*, vol. 18, no. 3, p. e0282674, 2023.
- [11] P. Kandula, M. Suin, and A. N. Rajagopalan, "Illumination-adaptive unpaired low-light enhancement," *IEEE Transactions on Circuits and Systems for Video Technology*, vol. 33, no. 8, pp. 3726–3736, 2023.
- [12] Y. Fu, Y. Hong, L. Chen, and S. You, "Le-gan: Unsupervised low-light image enhancement network using attention module and identity invariant loss," *Knowledge-Based Systems*, vol. 240, p. 108010, 2022.
- [13] L. Wang, L. Zhao, T. Zhong, and C. Wu, "Low-light image enhancement using generative adversarial networks," *Scientific Reports*, vol. 14, no. 1, p. 18489, 2024.
- [14] M. He, R. Wang, M. Zhang, F. Lv, Y. Wang, F. Zhou, and X. Bian, "Swinlightgan a study of low-light image enhancement algorithms using depth residuals and transformer techniques," *Scientific Reports*, vol. 15, no. 1, p. 12151, 2025.
- [15] F. Alhwarin, A. Ferrein, and I. Scholl, "Ir stereo kinect: improving depth images by combining structured light with ir stereo," in *Pacific Rim International Conference on Artificial Intelligence*. Springer, 2014, pp. 409–421.
- [16] J. Guan, R. Lai, A. Xiong, Z. Liu, and L. Gu, "Fixed pattern noise reduction for infrared images based on cascade residual attention cnn," *Neurocomputing*, vol. 377, pp. 301–313, 2020.
- [17] H. Lee and M. G. Kang, "Infrared image deconvolution considering fixed pattern noise," *Sensors*, vol. 23, no. 6, p. 3033, 2023.
- [18] A. Barral, P. Arias, and A. Davy, "Fixed pattern noise removal for multi-view single-sensor infrared camera," in *Proceedings of the IEEE/CVF Winter Conference on Applications of Computer Vision*, 2024, pp. 1669–1678.
- [19] O. Ronneberger, P. Fischer, and T. Brox, "U-net: Convolutional networks for biomedical image segmentation," in *International Conference on Medical image computing and computer-assisted intervention*. Springer, 2015, pp. 234–241.
- [20] X. Hu, M. A. Naiel, A. Wong, M. Lamm, and P. Fieguth, "Runet: A robust unet architecture for image super-resolution," in *Proceedings of the IEEE/CVF Conference on Computer Vision and Pattern Recognition Workshops*, 2019, pp. 0–0.
- [21] H. Zhang, Q. Lian, J. Zhao, Y. Wang, Y. Yang, and S. Feng, "Ratunet: residual u-net based on attention mechanism for image denoising," *PeerJ Computer Science*, vol. 8, p. e970, 2022.
- [22] Z. Wang, A. Bovik, H. Sheikh, and E. Simoncelli, "Image quality assessment: from error visibility to structural similarity," *IEEE Transactions on Image Processing*, vol. 13, no. 4, pp. 600–612, 2004.
- [23] J. Deng, W. Dong, R. Socher, L.-J. Li, K. Li, and L. Fei-Fei, "Imagenet: A large-scale hierarchical image database," in *2009 IEEE Conference on Computer Vision and Pattern Recognition*, 2009, pp. 248–255.
- [24] J. Johnson, A. Alahi, and L. Fei-Fei, "Perceptual losses for real-time style transfer and super-resolution," in *Computer Vision – ECCV 2016*, B. Leibe, J. Matas, N. Sebe, and M. Welling, Eds. Cham: Springer International Publishing, 2016, pp. 694–711.
- [25] Intel. (2020, Jun.) Intel® RealSense™ Product Family D400 Series Datasheet. Accessed: Dec. 10, 2024. [Online]. Available: <https://dev.intelrealsense.com/docs/intel-realsense-d400-series-product-family-datasheet>
- [26] R. Srikanth, B. Nagarjuna, K. Varshith, G. Supriya, and S. P. Reddy, "Enhancing of night time vehicle images using clahe method," in *2024 15th International Conference on Computing Communication and Networking Technologies (ICCCNT)*, 2024, pp. 1–8.
- [27] B. Cai, X. Xu, K. Guo, K. Jia, B. Hu, and D. Tao, "A joint intrinsic-extrinsic prior model for retinex," in *Proceedings of the IEEE International Conference on Computer Vision (ICCV)*, Oct 2017.
- [28] C. G. Guo, C. Li, J. Guo, C. C. Loy, J. Hou, S. Kwong, and R. Cong, "Zero-reference deep curve estimation for low-light image enhancement," in *Proceedings of the IEEE conference on computer vision and pattern recognition (CVPR)*, June 2020, pp. 1780–1789.
- [29] T. Wang, K. Zhang, T. Shen, W. Luo, B. Stenger, and T. Lu, "Ultra-high-definition low-light image enhancement: A benchmark and transformer-based method," in *Proceedings of the AAAI Conference on Artificial Intelligence*, vol. 37, no. 3, 2023, pp. 2654–2662.
- [30] Q. Yan, Y. Feng, C. Zhang, G. Pang, K. Shi, P. Wu, W. Dong, J. Sun, and Y. Zhang, "Hvi: A new color space for low-light image enhancement," *arXiv preprint arXiv:2502.20272*, 2025.
- [31] A. Ehambram, P. Hemme, and B. Wagner, "An approach to marker detection in ir- and rgb-images for an augmented reality marker," in *Proceedings of the 16th International Conference on Informatics in Control, Automation and Robotics - Volume 2: ICINCO, INSTICC, SciTePress*, 2019, pp. 190–197.
- [32] F. Shamsfakhr, A. Motroni, L. Palopoli, A. Buffi, P. Nepa, and D. Fontanelli, "Robot localisation using uhf-rfid tags: A kalman smoother approach †," *Sensors*, vol. 21, no. 3, 2021.
- [33] C. Campos, R. Elvira, J. J. G. Rodríguez, J. M. M. Montiel, and J. D. Tardós, "Orb-slam3: An accurate open-source library for visual, visual-inertial, and multimap slam," *IEEE Transactions on Robotics*, vol. 37, no. 6, pp. 1874–1890, 2021.
- [34] D. DeTone, T. Malisiewicz, and A. Rabinovich, "Superpoint: Self-supervised interest point detection and description," in *Proceedings of the IEEE conference on computer vision and pattern recognition workshops*, 2018, pp. 224–236.